

# Research on Eddy Current Field Characteristics of Eddy Current Displacement Sensor Based on ANSOFT

Yusheng Hu <sup>a,b</sup>, Jiqing Geng <sup>a,b</sup>, Weicai Huang <sup>a,b</sup>, Tuo Wang <sup>b</sup>

<sup>a</sup> State Key Laboratory of Air-conditioning Equipment and System Energy Conservation, Jinji West Road, Zhuhai City, Guangdong Province, China., wangtuo\_self@163.com

<sup>b</sup> Gree Electric Appliances. Inc. of Zhuhai, Jinji West Road, Zhuhai City, Guangdong Province, China.

**Abstract**—The eddy current field characteristics of the probe based on the eddy current magnetic field sensing principle of eddy current displacement sensor are the key to influence the performance of the sensor. In this paper, the eddy current field simulation of probe coils with different structures is performed. The effect of coil size and shape on the performance of the sensor is analyzed. The eddy current field characteristics of probe coils with different structures are studied. And build an experimental platform to test and analyze, verify the correctness of the simulation results, and lay the foundation for perfecting the eddy current displacement sensor theory and further optimization design.

## I. THEORETICAL RESEARCH AND SIMULATION ANALYSIS

### A. Test Theory of Eddy Current Displacement Sensor

The eddy current displacement sensor uses the eddy current effect to perform displacement test. According to Faraday's law of electromagnetic induction, when the sensor probe coil is connected to a sinusoidal alternating current  $i_1$ , a sinusoidal alternating magnetic field  $H_1$  is generated in the space around the coil, which causes the induced current on the surface of the measured metal conductor in the magnetic field, and also named eddy current<sup>[1]</sup>, as shown in Fig.1. At the same time, the electric eddy current  $i_2$  produces a new alternating magnetic field  $H_2$ , which is opposite to the direction of  $H_1$ , and the reverse magnetic field will weaken the  $H_1$ , thus the equivalent resistance of the probe coil will change correspondingly, and the displacement  $x$  can be measured by the change of the equivalent impedance  $Z$  in the control circuit.

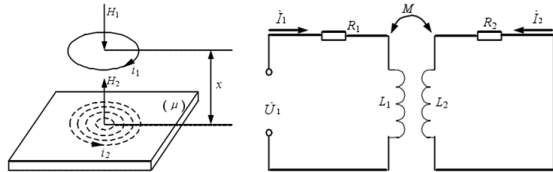


Fig.1 Schematic diagram and equivalent circuit diagram of eddy current displacement sensor

In the figure,  $R_1$  and  $L_1$  are the resistance and inductance of the sensor probe coil. The short-circuit ring can be considered as a short-circuit coil, where  $R_2$  and  $L_2$  are the resistance and inductance of the conductor under test. There is a mutual inductance  $M$  between the probe coil and the conductor, which increases as the distance between the coil and the conductor decreases.  $U_1$  is the excitation voltage. According to the Kirchhoff voltage balance equation, the equilibrium equation of the equivalent circuit in the figure above is as follows:

$$\begin{cases} R_2 \dot{I}_2 + j\omega L_2 \dot{I}_2 - j\omega M \dot{I}_1 = 0 \\ R_1 \dot{I}_1 + j\omega L_1 \dot{I}_1 - j\omega M \dot{I}_2 = \dot{U}_1 \end{cases}$$

By deriving a series of equations, the equivalent impedance  $Z$  of the probe coil can be expressed as the following function<sup>[2]</sup>:

$$Z_s = F(\sigma, \xi, \rho, \delta, I, \omega)$$

Where:  $\sigma$  --- conductor conductivity measured  
 $\xi$  --- The conductor permeability measured  
 $\rho$  --- coil size factor  
 $\delta$  --- Induction coil distance from measured metal surface  
 $I$  --- current intensity  
 $\omega$  --- excitation frequency

From the formula point of view, the main factors affecting the characteristics of the eddy current displacement sensor are the resistivity  $\sigma$  of the tested metal conductor, the permeability  $\xi$ , the coil size factor  $\rho$ , the distance  $\delta$  of the coil from the measured metal conductor, the current intensity  $I$ , and the excitation frequency  $\omega$ . This paper mainly studies the size factor  $\rho$  and the distance  $\delta$  from the induction coil to the metal conductor.

### B. Simulation Analysis Model

The main factor affecting the coil size factor is the size and shape of the coil. Combined with the installation size of the magnetic levitation sensor and the material of the measured shaft and other parameters, a simulation model was established in ANSOFT Maxwell, as shown in Fig.2 .

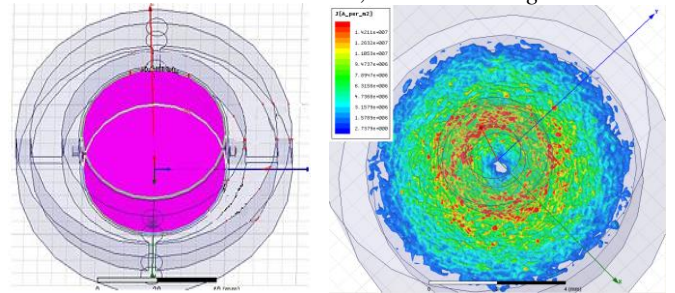


Fig.2 Simulation model of eddy current displacement sensor

#### a) Simulation analysis of cylindrical coils

The cylindrical coil is the most widely used sensor coil in the field of eddy current sensors. According to the mounting structure of the sensor of the magnetic levitation unit, parameters such as coil inner diameter  $a$ , outer diameter  $b$ , thickness  $c$ , and distance  $\delta$  between the coil and the metal

conductor are set, as shown in Fig.3 . The number of turns of the ampere turns should be calculated based on the cross-sectional area of the coil and the coil diameter, and the current and the excitation frequency should be constant.

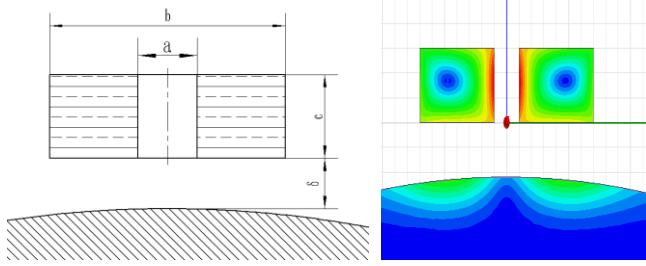
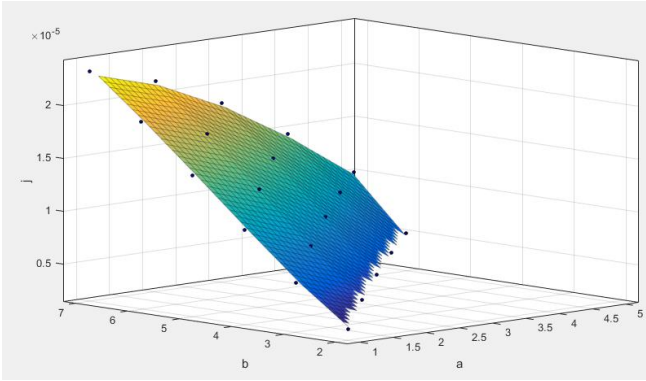


Fig.3 Simulation of cylindrical coil

Taking the inner diameter  $a$  of the coil, the outer diameter  $b$  and the distance  $\delta$  from the metal conductor of the coil as variables, the inductive eddy current density of the measured surface is simulated and the results are as follows:



$a$ : Coil inner diameter  $b$ :Coil outer diameter  $j$ :Magnetic density  
Fig.4 Simulation results of cylindrical coil

From the simulation results, we can draw the following conclusions:

1. When the distance  $\delta$  between the coil and the metallic conductor being measured is constant, the larger the cross-sectional area of the coil, the denser the induced eddy current field.
2. In the case of the same coil cross-sectional area, the larger the outer diameter of the coil, the greater the density of the induced eddy current field;
3. The greater the distance between the coil and the measured metal conductor  $\delta$ , the smaller the density of the induced eddy current field.

*b) Simulation analysis of trapezoidal coil*

Analysing the magnetic flux division of the cylindrical coil, it was found that the magnetic lines were mainly concentrated on the center of the coil and on the side close to the metal sensing surface. The magnetic field strength of the part far from the center of the coil and the part far from the tested metal conductor was low, so consider to adjust the shape of the coil to a trapezoidal coil for simulation analysis.

Taking the inner diameter of the coil  $a$ , the outer diameter  $b$  of the small end, the outer diameter  $d$  of the big end, and the distance  $\delta$  of the coil distance from the metal conductor as variables, the coil thickness  $c$  is a fixed value, and the simulated eddy current field density of the measured surface is simulated. As shown in Fig.5 .

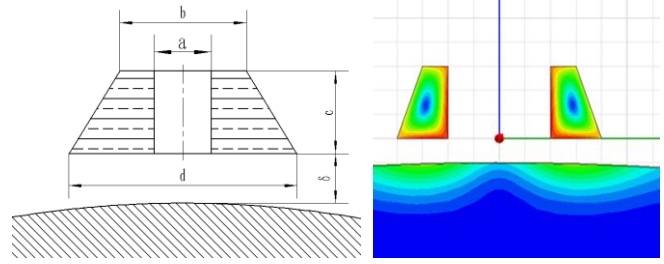


Fig.5 Simulation of trapezoidal coil

The comparison of the simulation results of the trapezoidal coil and the cylindrical coil is as follows:

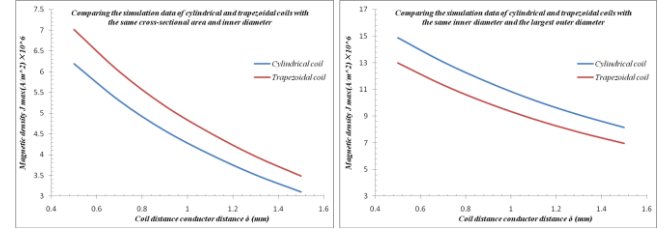


Fig.6. Comparison of simulation results for trapezoidal and cylindrical coils

From the simulation results, we can draw the following conclusions:

1. In the case of the same cross-sectional area and the same inner diameter, the current field density of the trapezoidal coil is larger than cylindrical coil;
2. In the same inner three-dimensional size (the same inner diameter, the same maximum outer diameter), current field density of trapezoidal coil is less than the cylindrical coil;

*c) Simulation analysis of hollow coil*

By analyzing the magnetic line division of the cylindrical coil, it is found that the magnetic field strength of the center part of the single-side coil is low, so consider the shape of the cylindrical coil is adjusted to a hollow coil for simulation analysis, that is, the coil center is filled with round plastic parts, it will be made hollow shape. As shown in Fig.7.

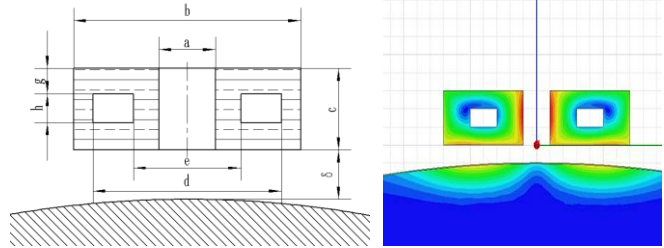


Fig.7 simulation of hollow coil

The three-dimensional dimension of the air coil is set to be the same as that of the cylindrical coil, and the simulated eddy current field density of the measured surface is simulated. The results are as follows:

| Type        | Inner-D /mm | Outer-D /mm | $\delta_1=0.5$ | $\delta_2=0.7$ | $\delta_3=0.9$ | $\delta_4=1.1$ | $\delta_5=1.3$ | $h=1.5$ | Amperes-turn A · N | Area mm <sup>2</sup> |
|-------------|-------------|-------------|----------------|----------------|----------------|----------------|----------------|---------|--------------------|----------------------|
| Cylindrical | 5           | 7           | 14.877         | 13.064         | 11.534         | 10.21          | 9.1038         | 8.157   | 114.5916           | 3                    |
|             | 7           | 7           | 23.263         | 20.874         | 18.818         | 16.86          | 15.283         | 13.899  | 171.8873           | 4.5                  |
| Trapezoida  | 1           | 7           | 20.977         | 18.667         | 16.617         | 14.86          | 13.388         | 8.003   | 114.6002           | 3                    |

Fig.8 Simulation data of the hollow coil

It can be seen from the simulation results that the induction eddy field density of the hollow coil is slightly lower than that of the columnar coil under the same three-dimensional size. Under the same cross section, the eddy current field density of the hollow coil is higher than that of the cylindrical coil.

## II. EXPERIMENTAL VERIFICATION

A magnetic suspension displacement sensor testing system is built based on Labview to realize automatic data recording and processing. As shown in Fig.9.

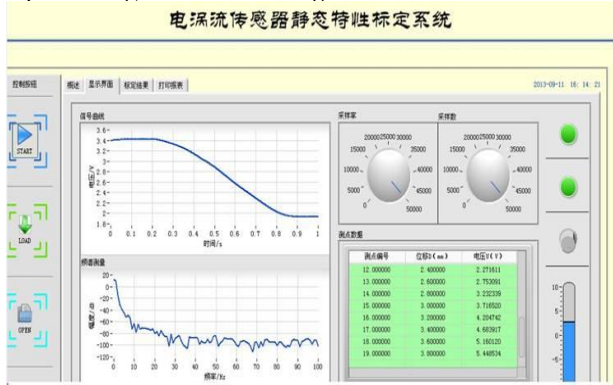


Fig. 9 The eddy current displacement sensor static calibration system operation interface

The wound coils of different sizes are assembled into the sensor housing, and the corresponding resonant voltage fluctuation value of the sensor is tested according to the requirements of the magnetic levitation unit on the starting point of the displacement sensor range.

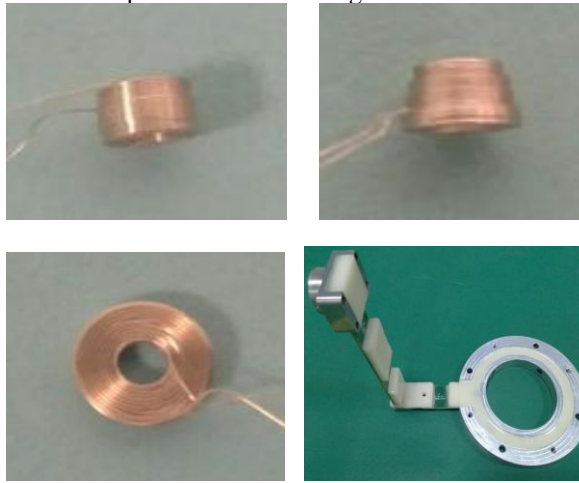


Fig.10 Schematic diagram of cylindrical coil, trapezoidal coil and hollow coil. Sensor conformation

| Type        | Inner-D /mm | Outer-D /mm      | $J_{max} (A/m^2) \times 10^6$ |                |                |                |                |           | Ampere-turn A · N | Area mm <sup>2</sup> |
|-------------|-------------|------------------|-------------------------------|----------------|----------------|----------------|----------------|-----------|-------------------|----------------------|
|             |             |                  | $\delta_1=0.5$                | $\delta_2=0.7$ | $\delta_3=0.9$ | $\delta_4=1.1$ | $\delta_5=1.3$ | $h_6=1.5$ |                   |                      |
| Cylindrical | 1           | 2                | 0.96121                       | 0.812858       | 0.69616        | 0.6061         | 0.528086       | 0.463524  | 5.15662           | 0.75                 |
|             |             | 3                | 2.35315                       | 2.013658       | 1.740134       | 1.521938       | 1.334674       | 1.178684  | 57.29578          | 1.5                  |
|             |             | 4                | 3.97214                       | 3.442496       | 3.005458       | 2.646358       | 2.338064       | 2.079626  | 85.94367          | 2.25                 |
|             |             | 5                | 5.65326                       | 4.96432        | 4.38292        | 3.8798         | 3.459444       | 3.09966   | 114.5916          | 3                    |
|             |             | 6                | 7.29562                       | 6.47938        | 5.7855         | 5.1509         | 4.63182        | 4.1819    | 143.2394          | 3.75                 |
|             |             | 7                | 8.83994                       | 7.93212        | 7.15084        | 6.4068         | 5.80754        | 5.28162   | 171.8873          | 4.5                  |
|             |             | Trapezoida (b=4) | 1                             | 5              | 4.93582        | 4.3092         | 3.784686       | 3.340276  | 2.96571           | 2.647422             |
| 6           | 5.85656     |                  |                               | 5.15394        | 4.56114        | 4.04016        | 3.606352       | 3.234066  | 114.5916          | 3                    |
| 7           | 6.71346     |                  |                               | 5.95726        | 5.31126        | 4.72416        | 4.24118        | 3.8228    | 128.9155          | 3.375                |
| Hollow      | 1           | 7                | 7.97126                       | 7.09346        | 6.31446        | 5.6468         | 5.08744        | 3.04114   | 143               | 3.75                 |

Fig.11 The test data of the resonant voltage of the coil

## III. DATA ANALYSIS

By analyzing the resonant voltage test data of coils of different sizes and shapes, it was found that the main factors influencing the coil eddy current field characteristics were the coil cross-sectional area, the maximum outer diameter of the

coil, and the distance of the coil from the measured metal conductor, and the law was also found:

- The larger the cross-sectional area of the coil (the smaller the inner diameter, the larger the outer diameter, and the thicker the thickness), the larger the resonant voltage;
- In the case of the same coil cross-sectional area, the larger the outer diameter of the coil, the greater its resonant voltage;
- The coil resonant voltage is inversely proportional to the distance  $\delta$  from the coil to the metal conductor under test;
- In the case of the same three-dimensional dimensions (with the same inner diameter, the same maximum outer diameter, and the same thickness), the order of coil resonant voltages is: columnar coils  $\geq$  hollow coils  $\geq$  trapezoidal coils;
- In the case of the same cross-sectional area and the same inner diameter, the amplitude of the resonant voltage fluctuation of the hollow coil is the largest;
- In the case of the same three-dimensional dimensions, setting a reasonable hollow size of the coil will have less influence on the magnetic field distribution of the coil and the density of the induced eddy current field.

## IV. SUMMARY

This paper studies the eddy current magnetic field characteristics and the main influencing factors of the probe coil. Through the eddy current field simulation of cylindrical coils, trapezoidal coils, and hollow coils of different sizes, the influence of coil size and shape on the sensor performance was analyzed. The experimental platform was set up for testing and analysis, and the correctness of the simulation results was verified, which laid the foundation for perfecting the theory of eddy current sensors and further optimizing the design.

## References

- Jae joon K, Guang Y ,Lalita U ,Satish U.Classification of pulsed eddy current GMR data on aircraft structures, 2010,43:141-144
- Hongbo W,Zhuhua F.Ultrastable and highly sensors eddy current displacement sensor using seif-temperature compensation.sensors and actuators,2013.203:362